Nano Today 48 (2023) 101695

Contents lists available at ScienceDirect

Nano Today

journal homepage: www.elsevier.com/locate/nanotoday

Negative thermal expansion behaviour of graphdiyne

Ya Kong [a,1], Yuling Yin [b,c,1], Xueting Feng [a], Zixuan Zhang [a], Feng Ding [b,c,*], Lianming Tong [a,**], Jin Zhang [a,**]

[a] Center for Nanochemistry, Beijing Science and Engineering Center for Nanocarbons, Beijing National Laboratory for Molecular Sciences, College of Chemistry and Molecular Engineering, Peking University, Beijing 100871, PR China
[b] Center for Multidimensional Carbon Materials, Institute for Basic Science (IBS), Ulsan 44919, the Republic of Korea
[c] Department of Materials Science and Engineering, Ulsan National Institute of Science and Technology (UNIST), Ulsan 44919, the Republic of Korea

ARTICLE INFO

Article history:
Received 27 July 2022
Received in revised form 31 October 2022
Accepted 15 November 2022
Available online xxxx

Keywords:
Negative thermal expansion (NTE)
Graphdiyne (GDY)
Raman spectroscopy

ABSTRACT

Negative thermal expansion (NTE) is an effect of a material contracting upon heating, and NTE materials are useful for the preparation of zero thermal expansion (ZTE) composite materials for applications in energy conversion and electronic devices. In this work, the NTE behaviour of graphdiyne (GDY) was observed and studied by temperature-dependent Raman spectroscopy. The characteristic Y mode in Raman spectra of GDY film exhibit blueshift with increasing temperature, in contrast to the redshift of positive thermal expansion materials. Our theoretical calculations show that the dimension of GDY decreases when the temperature is elevated, and the blueshift of the Y mode is due to the contraction of GDY. The thermal expansion coefficient (TEC) of GDY in the temperature range of 180–420 K was found to be negative, -7.18×10^{-6} K^{-1} at room temperature. Our results provide a measure of the thermal property of GDY and indicate promising applications of GDY in NTE composite materials.

Introduction

Negative thermal expansion (NTE) materials exhibit the behaviour of contraction by heating and expansion by cooling in a certain temperature range [1]. For example, water is a typical NTE material within the temperature range from 273 K to 277 K. It has been reported that NTE phenomena exist in ferroelectrics [2,3], semiconductors [4], superconductors [5] and magnetic materials [6]. Cubic zirconium tungstate, ZrW_2O_8, has been reported as a NTE material with a large NTE coefficient of -9.1×10^{-6} K^{-1} between a broad temperature range from 0.3 K to 1443 K since 1996 [7] and has been utilized to modify Si nanoparticles to decrease the volume change enhancing electrochemical performance and safety [8].

Carbon materials, such as fullerene, graphene, carbon nanotube (CNT) and graphyne (GY), possess NTE properties due to their special chemical structures [9–12]. For example, temperature-induced coupling between the soft vibration modes and shape changes plays a dominant role in NTE property of fullerenes [9]. The NTE behaviour of CNT bundles is confirmed by bending of the CNT walls and the elliptization of the CNT cross section induced by thermal fluctuations [10]. The NTE phenomenon of graphene stems from the ripple effect [13]. GY is a two-dimensional (2D) carbon materials consisted of sp- and sp^2- hybridized carbon atoms. Benefiting from the uniform pore structure and flexible links between benzene units, the NTE behaviour of GY can be induced by both the ripple effect and the rigid unit modes (RUMs) [11,12] similar to other framework structure materials such as ZrW_2O_8 [14]. Graphdiyne (GDY) is the most studied structure in GY family, and the composite materials of GDY have shown important applications in many fields such as energy storage and conversion [15,16], photo-electrical device [17], biomedicine [18–20], etc. However, the thermal expansion property of GDY, which is extremely significative for the applications of GDY composite materials, has not been explored yet.

Raman spectroscopy is a useful tool to explore the structural and electron-phonon properties of nanomaterials [21–23]. Besides, the thermal properties of materials, especially 2D materials, can also be monitored by Raman spectroscopy. The thermal conductivity of a suspended single-layer graphene can be measured by monitoring the Raman G band [23,24]. The extracted thermal conductivity at room temperature is in the range of $4.84 \pm 0.44 \times 10^3$ to $5.30 \pm 0.48 \times 10^3$ Wm^{-1} K^{-1}. The thermal expansion coefficient (TEC)

* Corresponding author at: Center for Multidimensional Carbon Materials, Institute for Basic Science (IBS), Ulsan 44919, the Republic of Korea
** Corresponding authors.
E-mail addresses: f.ding@unist.ac.kr (F. Ding), tonglm@pku.edu.cn (L. Tong), jinzhang@pku.edu.cn (J. Zhang).
[1] Equal contributions.

https://doi.org/10.1016/j.nantod.2022.101695
1748-0132/

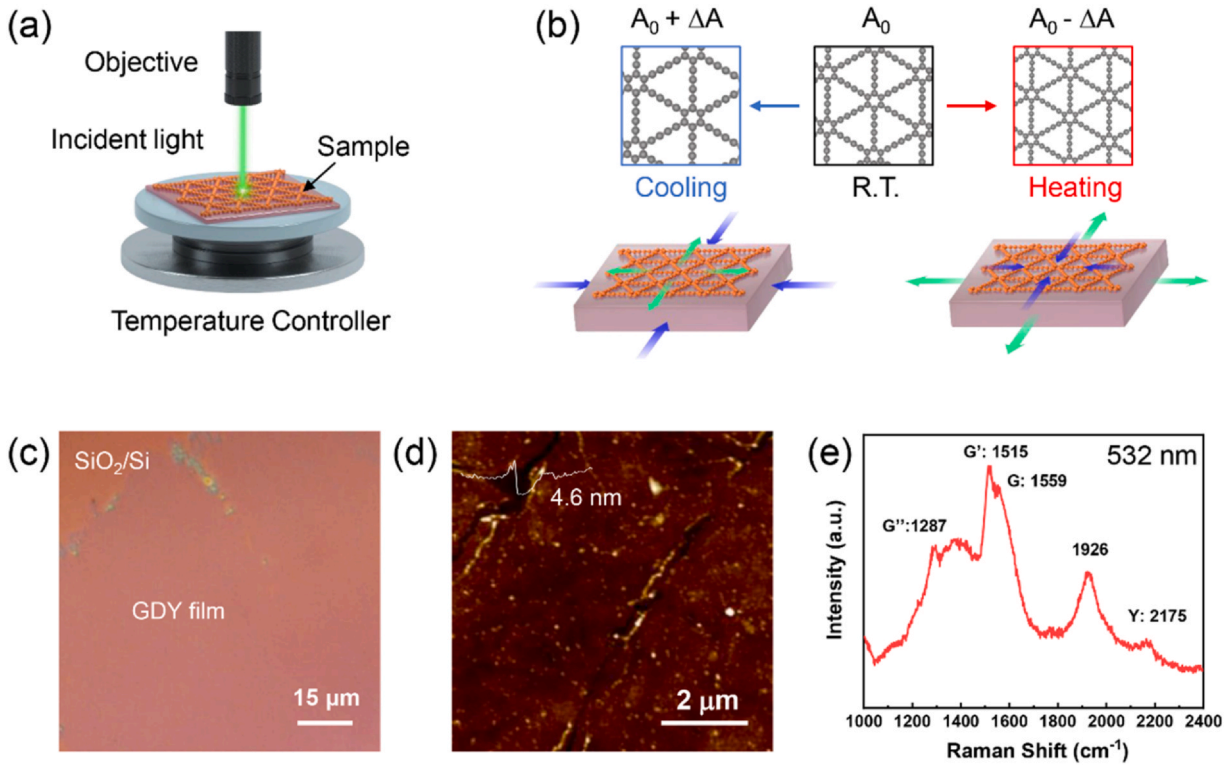

Fig. 1. (a) Schematic illustration of *in-situ* Raman measurement for GDY film. (b) Schematic illustration of thermal expansion and contraction of GDY on a SiO_2/Si substrate during cooling and heating processes. (blue arrows: contraction; green arrows: expansion) (c) Optical microscope (OM) image of GDY film on SiO_2/Si substrate. (d) Atomic force microscope (AFM) image of GDY film. (e) Raman spectrum of GDY film on SiO_2/Si substrate collected using 532 nm laser at room temperature.

of graphene on a SiO_2/Si substrate can also be roughly measured by means of temperature-dependent Raman spectroscopy, which is about -8.0×10^{-6} K^{-1} at room temperature [25].

Here, we investigated the NTE behaviour of GDY and estimated its TEC in the temperature range of 170–430 K characterized by Raman spectroscopy. The observed NTE behaviour of GDY film on SiO_2/Si substrate was found to originate from two effects: the intrinsic NTE property of GDY and the strain caused by thermal expansion mismatch between GDY and the substrate. Our theoretical calculations show that the NTE effect of GDY originates from the redshifts of low frequency phonon modes in GDY upon compression and the NTE mechanism is identified as RUMs which is similar to ZrW_2O_8. Both experimental data and theoretical calculation results verified the blueshift of the Y Raman mode with increasing temperature. The experimental value of TEC is approximately -7.18×10^{-6} K^{-1} at room temperature. Our findings reveal the intrinsic thermal property of GDY and indicate an advantageous function of thermal response in GDY composite materials.

Result and discussion

The GDY film was synthesized according to our previous work [26], and the film was then transferred onto a 300 nm SiO_2/Si substrate. Raman spectra were measured using a confocal Raman spectrometer with a temperature controller under inert gas atmosphere as shown in Fig. 1a. When the temperature is raised or declined, both the lattice variation of the GDY film and the volume change of substrate should be considered, as schematically shown in Fig. 1b. Due to the discrepancy in TEC between GDY film and the substrate, additional strain is exerted to GDY film. It has been reported that two effects, the temperature-dependent phonon frequencies and the modification of the phonon dispersion caused by strain, lead to the shift of Raman peaks [25,27]. Fig. 1c shows the optical microscope (OM) image of GDY film on a SiO_2/Si substrate. The thickness of the GDY film is about 4.6 nm measured by atomic force microscope (AFM) as shown in Fig. 1d. The Raman spectrum of GDY film exhibits five typical peaks in the range of 1000–2400 cm^{-1} in agreement with theoretical predictions (Fig. 1e) [27,28]. The G (at 1559 cm^{-1}), G′ (at 1515 cm^{-1}) and G′′ (at 1287 cm^{-1}) peaks are related to the vibrations of sp^2-carbon, and the Y peak (at 2175 cm^{-1}) is attributed to the alkyne-related modes. The peak at 1926 cm^{-1} is usually assigned to the vibration of intermediate $C_6H_5C{\equiv}CCu$ [27].

Temperature-dependent Raman spectra between 170 K and 430 K are displayed in Fig. 2. All peaks show a significant decrease in intensity and broadening with increasing temperature (Fig. 2a). Fig. 2b shows the fitted Y peak at different temperatures, where a distinct blueshift is observed as the temperature gradually increases, in contrast to the redshift of positive thermal expansion 2D materials [29]. The results in Fig. 2c show the frequency shift of the Y band as a function of temperature. The relative Raman shifts $\Delta\omega/\omega_0$ to the reference at T = 300 K are exhibited in Fig. 2d. The peak positions were fitted as a polynomial function of temperature according to the phonon–phonon coupling, which leads to the nonlinear temperature dependent behaviour of the Raman peaks [22]. Therefore the temperature-dependent Y peak position can be fitted using a second-order polynomial function of temperature (T):

$$\omega(T) = \omega_0 + B_1 T + B_2 T^2 \quad (1)$$

where, ω_0 is the Y peak position at 0 K; B_1 and B_2 are the first- and second-order coefficients, respectively. The fitting parameters of ω_0, B_1 and B_2 are 2156.4 cm^{-1}, 0.0855 cm^{-1} K^{-1} and -7.09×10^{-5} cm^{-1} K^{-2}, respectively. The positive first-order coefficient strongly indicates that GDY is a NTE material.

In order to elucidate the origin of the NTE property, we calculated the Helmholtz free energy (F) of GDY as a function of the temperature (T) and the area of a unit cell (A). The computational results are plotted as a color-coded map shown in Fig. 3a, where the color represents the change of Helmholtz free energy difference (ΔF) with

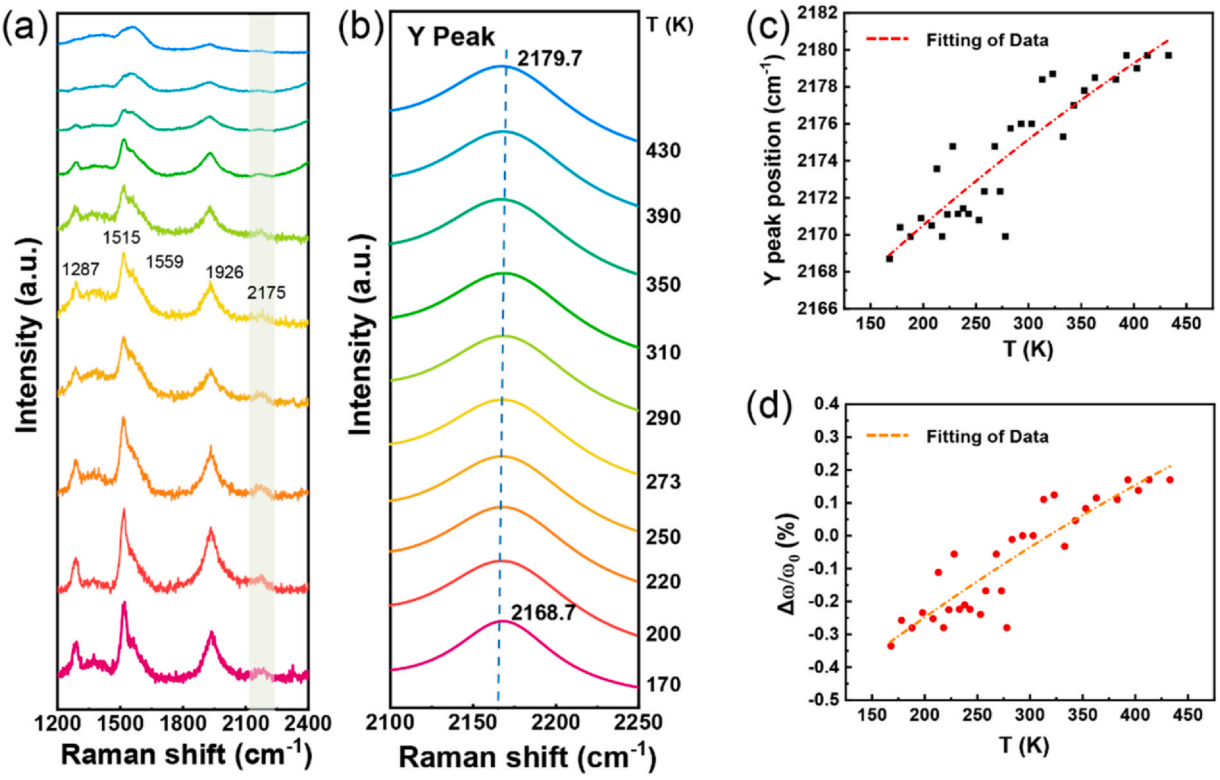

Fig. 2. (a) Temperature dependent Raman spectra of GDY. (b) The fitted Y peak at different temperatures. (c) Raman frequency shifts of the Y peak as a function of temperature. (d) The relative Raman shift $\Delta\omega/\omega_0$ to the reference at T = 300 K.

respect to the minimum at a specific temperature. From the color map, we can clearly see that, as the temperature increases, the location of $\Delta F = 0$ moves to smaller A. This indicates the lattice of GDY will contract at a higher temperature and the GDY has a negative thermal expansion coefficient. We plot the area of GDY unit cell as a function of the temperature, which corresponds to the black line of $\Delta F = 0$ in Fig. 3a. The negative thermal expansion behaviour in a very broad temperature range is clearly shown in Fig. 3b. A_0 is the area of unit cell of GDY at 0 K and $\Delta A = A - A_0$ is the change of A. It is seen that the area of GDY contracts rapidly by 1.4 % from 0 K to 500 K, and then the contraction becomes slower from 500 K to 1000 K. The absolute value of A as a function of T was plotted in Fig. S2. The results presented here are consistent with theoretical calculations for α-graphyne, β-graphyne and γ-graphyne in a previous study [11]. The TEC of GDY is calculated and shown as the red curve in Fig. 3b. A negative value is seen over the range of 0–1000 K, decreases significantly from 0 K to 130 K, and increases at higher temperatures. The minimum value was observed at 130 K and is about -4.81×10^{-5} K^{-1}.

The blueshift of Y mode in Raman spectra of GDY can be explained by the contraction of material with increasing temperature. Fig. 4a and S3 show the phonon dispersion relations of GDY at − 1 %, − 0.5 %, 0 %, 0.5 % and 1 % strain, where negative strain corresponds contraction and positive strain corresponds expansion. All the high frequency modes, including the Y mode, blueshift with the increase of compressive strain and redshift with the increase of tensile strain. Fig. 4b shows the linear relationship between Raman frequency of the Y mode and the area of unit cell, where ω_0 is the frequency of Y peak at 0 K and $\Delta\omega = \omega - \omega_0$ is the frequency shift. $\Delta\omega/\omega_0$ drops linearly with $\Delta A/A_0$ and the slope is ~ − 1.36. In contrast to the blueshift of high frequency phonons, upon compression, the low frequency phonons redshift or the density of states (DOS) of low frequency phonons becomes rich. At a higher temperature, the Helmholtz free energy contribution by low frequency phonons increase drastically

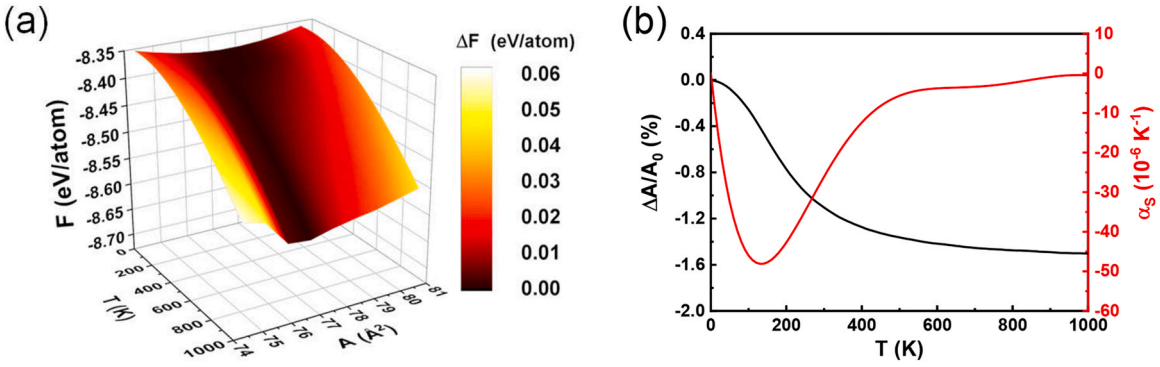

Fig. 3. (a) Helmholtz free energy as a function of temperature and unit cell area of GDY, where $\Delta F(T, A) \equiv F(T, A) - \min_A F(T, A)$, the free energy difference with respect to the minimum value for a given temperature, is depicted by the color-coded map. (b) Temperature dependence of the ratio of area expansion to the reference area at T = 0 K (black line) and the corresponding area thermal expansion coefficient (red line).

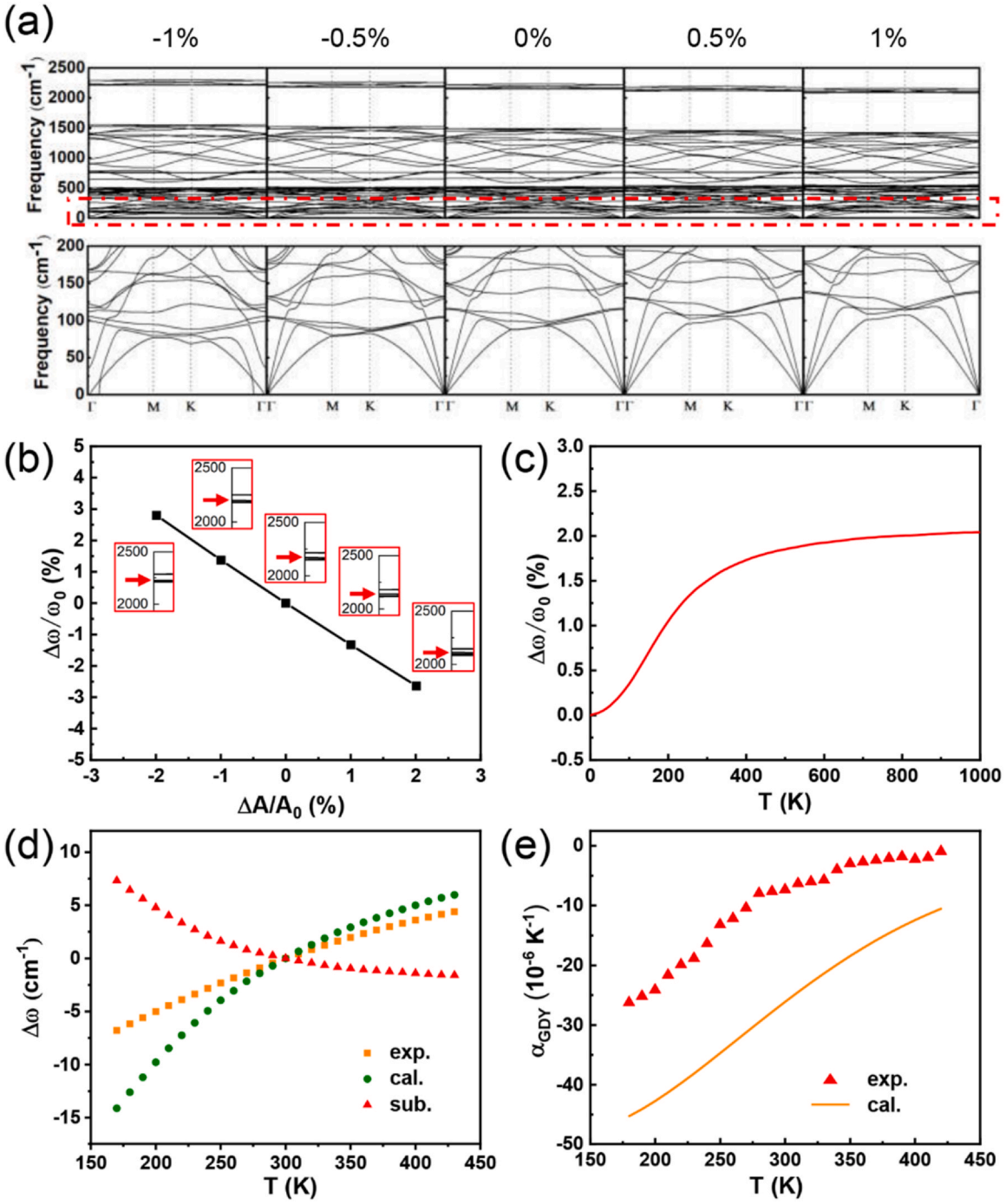

Fig. 4. (a) The phonon dispersion relations under strain of GDY along the high symmetry lines in 2D hexagonal Brillouin zones. (b) Raman frequency shifts of Y peak as a function of the unit cell area. (c) Theoretically calculated temperature dependent Y peak frequency of GDY. (d) The relative Raman shift of Y peak as a function of temperature. Yellow square: experimental data, $\Delta\omega^{exp.}$; green dot: theoretically calculated data, $\Delta\omega^{cal.}$; red triangle: estimated data induced by strain, $\Delta\omega^{sub.} = \Delta\omega^{exp.} - \Delta\omega^{cal.}$. (e) Experimental (red triangle) and theoretically calculated (yellow line) thermal expansion coefficient of GDY.

(Eq. (S1)) and thus, the enrichment of the low-frequency DOS by the contraction of the GDY leads to a more stable structure [30]. The corresponding $\Delta\omega/\omega_0$ versus temperature was plotted in Fig. 4c, where $\Delta\omega/\omega_0$ increases rapidly from 0 K to 500 K and then becomes slower and slower from 500 K to 1000 K. This trend is the opposite of area strain $\Delta A/A_0$ versus temperature T, as $\Delta\omega/\omega_0$ is inversely proportional to $\Delta A/A_0$.

According to the previous study [25], the temperature-dependent Raman frequency shifts of freestanding GDY, $\Delta\omega^{F}_{GDY}(T)$, can be majorly attributed by two factors: thermal expansion of the lattice, $\Delta\omega^{E}(T)$, and the anharmonic effect, $\Delta\omega^{A}(T)$, which changes the phonon self-energy. Therefore, $\Delta\omega^{F}_{GDY}(T)$ can be expressed as:

$$\Delta\omega^{F}_{GDY}(T) = \Delta\omega^{E}(T) + \Delta\omega^{A}(T) \quad (2)$$

It should be noted that our GDY sample is on the SiO_2/Si substrate, so the Raman shift resulted from the substrate, $\Delta\omega^{sub.}(T)$, should be included. Based on the assumptions of strong van der Waals (vdW) interaction and the strain effect between the substrate and the sample, the temperature-dependent Raman shifts of supported GDY, $\Delta\omega^{sup.}_{GDY}(T)$, can be written as:

$$\Delta\omega_{GDY}^{sup.}(T) = \Delta\omega^{E}(T) + \Delta\omega^{A}(T) + \Delta\omega^{sub.}(T) \quad (3)$$

Since $\Delta\omega^{sub.}(T)$ is related to the strain effect caused by the TEC mismatch between the material and the substrate, $\Delta\omega^{sub.}(T)$ can be expressed as:

$$\Delta\omega^{sub.}(T) = \beta\int_{T_0}^{T}\left[\alpha_{SiO_2}(T) - \alpha_{GDY}(T)\right] \quad (4)$$

where β is the biaxial strain coefficient of GDY, and α_{SiO_2} and α_{GDY} are the TEC values of SiO_2 and GDY, respectively. The value of β was chosen as $-32.9\,cm^{-1}/\%$ [27] and the temperature-dependent values of α_{SiO_2} can be found from literature [31] for calculating TEC of GDY in this work.

Fig. 4d shows the experimental (yellow squares) and calculated (green circles) Δω values (Y peak positions at *T* relative to the value at 300 K). Here, the experimental data of Raman shift $\Delta\omega^{exp.}(T)$ was considered as $\Delta\omega_{GDY}^{sup.}(T)$. As the Raman shift for freestanding GDY was not available, the theoretically calculated data $\Delta\omega^{cal.}(T)$ was used as $\Delta\omega_{GDY}^{F}(T)$. Therefore, the Raman shift induced by the substrate can be expressed as:

$$\Delta\omega^{sub.}(T) = \Delta\omega^{exp.}(T) - \Delta\omega^{cal.}(T) \quad (5)$$

which are plotted in Fig. 4d (red triangles). Finally, according to Eq. (4), the $\alpha_{GDY}(T)$ can be calculated by:

$$\alpha_{GDY}(T) = \alpha_{SiO_2}(T) - \frac{\delta\left[\frac{\Delta\omega^{Sub.}(T)}{\beta}\right]}{\delta T} \quad (6)$$

The results are presented in Fig. 4e. It is clear that the experimental data (red triangle) of TEC are negative at the measured temperature range between 180 K and 420 K, and agree well with the theoretical results (yellow line). The experimental and theoretical values of TEC at room temperature are approximately $-7.18\times10^{-6}\ K^{-1}$ and $-26.1\times10^{-6}\ K^{-1}$, respectively. The discrepancy between experimental and theoretical values may due to the facts that the GDY film contains multiple layers and the film is not freestanding.

Similar results were also obtained for GDY film directly grown on the polyacrylamide (PAAM) hydrogel (GDY/PAAM). The Raman spectra of GDY/PAAM at room temperature were measured and shown in Fig. S4. Since the water contained in the hydrogel evaporates during the heating process, we only measured the temperature-dependent Raman spectra below room temperature (Fig. S5). By fitting the Y peak positions, the findings are directly in line with the sample of GDY film on SiO_2/Si substrate (Fig. S6). The fitting parameters of ω_0, B_1 and B_2 are $2039.6\,cm^{-1}$, $0.838\,cm^{-1}\ K^{-1}$ and $-1.22\times10^{-3}\ cm^{-1}\ K^{-2}$, respectively. The blueshift of Y peak is more pronounced than GDY film on SiO_2/Si substrate, which may be due to the expansion of hydrogel [32].

Conclusion

In conclusion, we have explored the negative thermal expansion behaviour of GDY by temperature-dependent Raman spectroscopy and density functional calculations. The TEC of GDY film supported on SiO_2/Si substrate was estimated between the temperature range of 180–420 K, agree well with the results of DFT calculations. Negative TEC values were found and the TEC of GDY film at room temperature was calculated to be approximately $-7.18\times10^{-6}\ K^{-1}$. Our theoretical calculations indicate that the NTE effect is a consequence of the red shift of low frequency phonon modes upon material contraction, and the theoretical TEC values are in good agreement with the experimentally observed ones. These findings reveal the thermal expansion property of GDY and indicate useful applications of GDY composite as ZTE materials.

CRediT authorship contribution statement

Ya Kong: Conceptualization, Methodology, Formal analysis, Investigation, Resources, Writing – original draft. **Yuling Yin:** Methodology, Software, Formal analysis, Validation, Writing – original draft. **Xueting Feng:** Writing – original draft. **Zixuan Zhang:** Writing – original draft. **Feng Ding:** Methodology, Software, Formal analysis, Writing – review & editing, Supervision, Funding acquisition. **Lianming Tong:** Conceptualization, Methodology, Formal analysis, Writing – review & editing, Supervision, Funding acquisition. **Jin Zhang:** Conceptualization, Methodology, Formal analysis, Writing – review & editing, Supervision, Funding acquisition.

Data Availability

Data will be made available on request.

Declaration of Competing Interest

The authors declare that they have no known competing financial interests or personal relationships that could have appeared to influence the work reported in this paper.

Acknowledgements

We thank Dr. Shishu Zhang, Dr. Yan Zhao and Prof. Wei Hu for their helpful discussions. This work was financially supported by the Ministry of Science and Technology of China (2018YFA0703502 and 2016YFA0200100), the National Natural Science Foundation of China (Grant nos. 52021006, 51720105003, 21790052, 21974004), the Strategic Priority Research Program of CAS (XDB36030100), and the Beijing National Laboratory for Molecular Sciences (BNLMS-CXTD-202001). The authors acknowledge the support from the Institute for Basic Science (IBS-R019-D1) of Korea and the computational resources from CMCM, IBS.

Appendix A. Supporting information

Supplementary data associated with this article can be found in the online version at doi:10.1016/j.nantod.2022.101695.

References

[1] J. Chen, L. Hu, J. Deng, X. Xing, Chem. Soc. Rev. 44 (2015) 3522–3567.
[2] A.S. Bhalla, R. Guo, L.E. Cross, G. Burns, F.H. Dacol, R.R. Neurgaonkar, Phys. Rev. B 36 (1987) 2030–2035.
[3] S.B. Qadri, J.A. Bellotti, A. Garzarella, D.H. Wu, Appl. Phys. Lett. 86 (2005) 251914.
[4] C.H. Xu, C.Z. Wang, C.T. Chan, K.M. Ho, Phys. Rev. B 43 (1991) 5024–5027.
[5] J.J. Neumeier, T. Tomita, M. Debessai, J.S. Schilling, P.W. Barnes, D.G. Hinks, J.D. Jorgensen, Phys. Rev. B 72 (2005) 220505.
[6] K. Takenaka, H. Takagi, Appl. Phys. Lett. 87 (2005) 261902.
[7] T.A. Mary, S.O. Evans, T. Vogt, A.W. Sleight, Science 272 (1996) 90–92.
[8] N. Jing, S. Xu, Z. Wang, G. Wang, ACS Appl. Mater. Interfaces 13 (2021) 30468–30478.
[9] Y.K. Kwon, S. Berber, D. Toma´nek, Phys. Rev. Lett. 92 (2004) 015901.
[10] L.K. Galiakhmetova, E.A. Korznikova, A.A. Kudreyko, S.V. Dmitriev, Phys. Status Solidi RRL 16 (2022) 2100415.
[11] C.W. Kim, S.H. Kang, Y.K. Kwon, Phys. Rev. B 92 (2015) 245232.
[12] S.A. Hernandez, A.F. Fonseca, Diam. Relat. Mater. 77 (2017) 57–64.
[13] W. Bao, F. Miao, Z. Chen, H. Zhang, W. Jang, C. Dames, C.N. Lau, Nat. Nanotechnol. 4 (2009) 562–566.
[14] F. Bridges, T. Keiber, P. Juhas, S.J.L. Billinge, L. Sutton, J. Wilde, G.R. Kowach, Phys. Rev. Lett. 112 (2014) 045505.
[15] N. Wang, J. He, K. Wang, Y. Zhao, T. Jiu, C. Huang, Y. Li, Adv. Mater. 31 (2019) 1803202.
[16] X. Chen, X. Jiang, N. Yang, Small (2022) 2201135.
[17] J. Guo, R. Shi, R. Wang, Y. Wang, F. Zhang, C. Wang, H. Chen, C. Ma, Z. Wang, Y. Ge, Y. Song, Z. Luo, D. Fan, X. Jiang, J. Xu, H. Zhang, Laser Photon. Rev. 14 (2020) 1900367.
[18] S. Li, Y. Chen, H. Liu, Y. Wang, L. Liu, F. Lv, Y. Li, S. Wang, Chem. Mater. 29 (2017) 6087–6094.
[19] J. Liu, C. Chen, Y. Zhao, Adv. Mater. (2019) 1804386.

[20] R. Wang, M. Shi, F. Xu, Y. Qiu, P. Zhang, K. Shen, Q. Zhao, J. Yu, Y. Zhang, Nat. Commun. 11 (2020) 4465.
[21] C. Zhou, Q. Zhang, M. Zhang, G. Wu, J. Alloy. Compd. 718 (2017) 365e360.
[22] Z. Lin, W. Liu, S. Tian, K. Zhu, Y. Huang, YangYang, Sci. Rep. 11 (2021) 7073.
[23] I. Calizo, A.A. Balandin, W. Bao, F. Miao, C.N. Lau, Nano Lett. 7 (2007) 2645–2649.
[24] A.A. Balandin, S. Ghosh, I.C. Wenzhong Baoȝ, D. Teweldebrhan, F. Miao, C.N. Lau, Nano Lett. 8 (2008) 902–907.
[25] D. Yoon, Y.W. Son, H. Cheong, Nano Lett. 11 (2011) 3227–3231.
[26] Y. Kong, X. Li, L. Wang, Z. Zhang, X. Feng, J. Liu, C. Chen, L. Tong, J. Zhang, ACS Nano 16 (2022) 11338–11345.
[27] S. Zhang, J. Wang, Z. Li, R. Zhao, L. Tong, Z. Liu, J. Zhang, Z. Liu, J. Phys. Chem. C 120 (2016) 10605–10613.
[28] J. Wang, S. Zhang, J. Zhou, R. Liu, R. Du, H. Xu, Z. Liu, J. Zhang, Z. Liu, Phys. Chem. Chem. Phys. 16 (2014) 11303–11309.
[29] H. Zobeiri, S. Xu, Y. Yue, Q. Zhang, Y. Xie, X. Wang, Nanoscale 12 (2020) 6064–6078.
[30] P. Roy, E. Brueck, R. Groot, Phys. Rev. B 93 (2016) 165101.
[31] Standard Reference Material 739 Certificate, National Institute of Standards and Technology, Gaithersburg, MD, 1991.
[32] D.K. Aktaş, G.A. Evingür, Ö. Pekcan, J. Mater. Sci. 42 (2007) 8481–8488.